

# Effects of Al content on friction and wear behavior of weld surfacing Mg-Al-Zn alloy

Q. Chen<sup>1\*</sup>, Z. Zhao<sup>2</sup>, Z. Zheng<sup>1</sup>, G. Cheng<sup>1</sup>, Y. Zhao<sup>1</sup>, L. Lu<sup>1</sup>

<sup>1</sup>*School of Mechanical and Electronic Engineering, Shandong Jianzhu University, Jinan 250101, P. R. China*

<sup>2</sup>*School of Materials Science & Engineering, Northeastern University, Shenyang 110819, P. R. China*

Received 1 July 2019, received in revised form 3 October 2019, accepted 25 October 2019

## Abstract

In this study, surfacing-welding magnesium alloys with different compositions were prepared by changing the Al content in the Mg-Al-Zn alloy welding wire. Also, the effects of the Al content on the dry sliding tribological performance and wear mechanism at room temperature were investigated. The results revealed that the macro-hardness of the surfacing-welding Mg-Al-Zn alloy gradually increases. Also, the coefficient of friction and wear rate gradually decreases with the increase in the Al content from 3 to 9 % within the parameter range. Among these alloys, the surfacing-welding alloy containing 9 % Al exhibited the best wear resistance. The mechanism revealed that with the increase in the Al content, the grain size and amount of the  $\beta$ -Mg<sub>17</sub>Al<sub>12</sub> phase in the alloy gradually increased, and the phase evolved into a reticular shape from the originally dispersed particles. During the wear process, the reticular phase can resist the plowing action caused by microscopic hard protrusions on the grinding disc and the wear debris, protect the  $\alpha$ -Mg matrix, decrease the amount of fine granular debris generated by the abrasive wear mechanism, and enhance the wear resistance of the surfacing-welding alloy. Four wear mechanisms were observed during the friction and wear process of the surfacing-welding Mg-Al-Zn alloy, among which the abrasive wear and plastic extrusion of the surface metal were the principal wear mechanisms, while the oxidative wear and delamination wear were the secondary wear mechanisms.

**Key words:** surfacing welding, Mg-Al-Zn, magnesium alloy, friction and wear, wear resistance

## 1. Introduction

Owing to its high specific strength and good shock absorption, magnesium alloy has been considered as a lightweight material with high development potential, and it has been considerably applied in automobile manufacturing, aerospace, and other fields in recent years [1–3]. However, magnesium alloys also exhibit some limitations, such as low hardness prone to wear and scratch and high chemical activity prone to corrosion, easily leading to various local damage such as wear, abrasion, and corrosion during the service life of magnesium alloy components and parts. As a conventional surface cladding technology, surfacing welding can effectively and rapidly repair damaged magnesium alloy materials and can be employed for the surface strengthening and rapid prototyping of components

and parts; hence, this method is of significance in decreasing the manufacture and maintenance cycle, extending the service life of metal materials, and saving resources [4, 5]. Besides, owing to the flexible/simple operation and high repair efficiency, the surfacing welding technology demonstrates extremely important applications under some special circumstances, including the rapid emergency repair of weapons and equipment [6, 7].

As one of the basic failure forms of components, wear adversely affects the service state of magnesium alloy materials. Therefore, the friction and wear behavior of magnesium alloys have gradually become hot research topics in recent years. For example, Niu et al. have investigated the effects of test parameters such as test load, sliding speed, and ambient temperature on the friction and wear behavior of magnesium alloys

\*Corresponding author: e-mail address: [sideqq@163.com](mailto:sideqq@163.com)

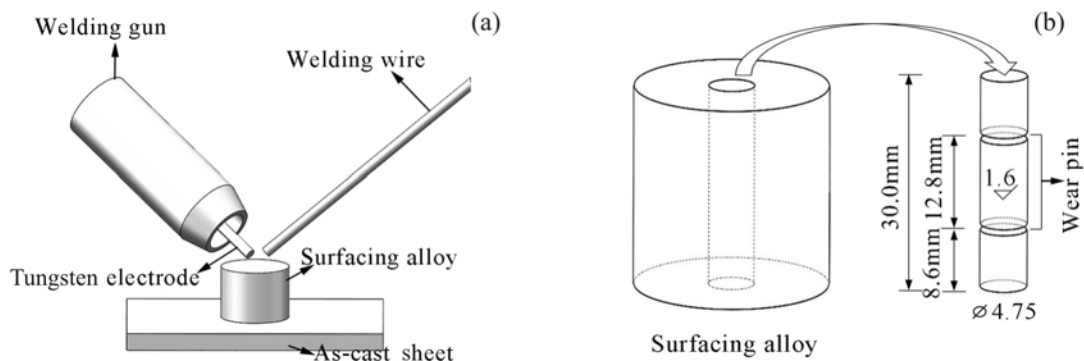


Fig. 1. Schematic of the surfacing-welding test [15].

Table 1. Chemical composition of the Mg-Al-Zn alloy welding wire (mass fraction)

Alloy	Al	Zn	Mn	Mg
AZ31	3.08	0.95	0.26	Bal.
AZ61	5.93	0.98	0.24	Bal.
AZ91	8.64	0.90	0.28	Bal.

and determined the wear mechanism of the Mg-3Al-0.4Si alloy under different test conditions [8, 9]. Hu et al. have investigated the effect of large deformation processing, such as high-pressure torsion on the tribological behavior of magnesium alloys [10, 11]. Yagi et al. have reported that the addition of rare earth elements such as Y and Gd can effectively enhance the wear resistance of magnesium alloys [12–14].

The wear resistance of the surfacing-welding magnesium alloy mainly depends on the welding material and welding process. The composition of the material (i.e., welding wire) used in surfacing welding is the basis for determining the post-welding performance. However, extremely few studies on the friction and wear behavior of surfacing-welding magnesium alloys and the relationship between the friction and wear behavior and the composition of the wire have been reported. The intrinsic relationship between the composition, wear mechanism and wear resistance of the alloy still needs systematic and intensive studies. Therefore, the effects of the variation of the Al content on the microstructure, tribological behavior, and wear mechanism of the surfacing-welding Mg-Al-Zn alloy are investigated by using a conventional Mg-Al-Zn magnesium alloy welding wire. The study can provide a basis for the composition design of the welding filling material comprising the magnesium alloy.

## 2. Experimental materials and methods

In this test, the diameter of the magnesium alloy

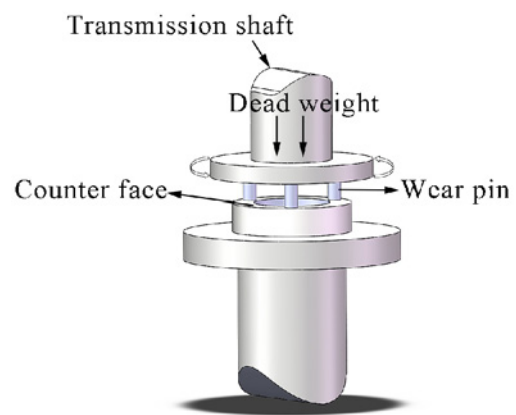


Fig. 2. Schematic of the pin-disc friction and wear test [15].

wire was 2.5 mm. Table 1 summarizes the chemical composition of the alloy wire. The thickness of the as-cast sheet material was 10 mm, and the composition consistent with that of the wire was used as the base material for welding. Before the welding test, the oxide films on the surfaces of the base metal and wire were removed by mechanical grinding, and then the surfaces were washed using an organic solvent such as alcohol. Surfacing welding was carried out on a magnesium alloy sheet surface by tungsten-inert gas-shielded welding. The diameter and height of the specimen were 20 and 30 mm, respectively. Figure 1a shows the schematic diagram of the surfacing-welding process. The welding voltage was 15 V, the current was 130 A, the protection gas was argon with a purity of 99.99 %, and the flow rate was 16 L min<sup>-1</sup>. After the surfacing-welding test, the specimen was cut along its longitudinal section by wire cutting, and the section was mechanically polished. The microstructures were observed by optical microscopy (DMI5000M, Leica) and scanning electron microscopy (SEM, SSX-550, SHIMADZU). The phase composition of the surfacing-welding alloy was analyzed by X-ray diffraction (XRD,

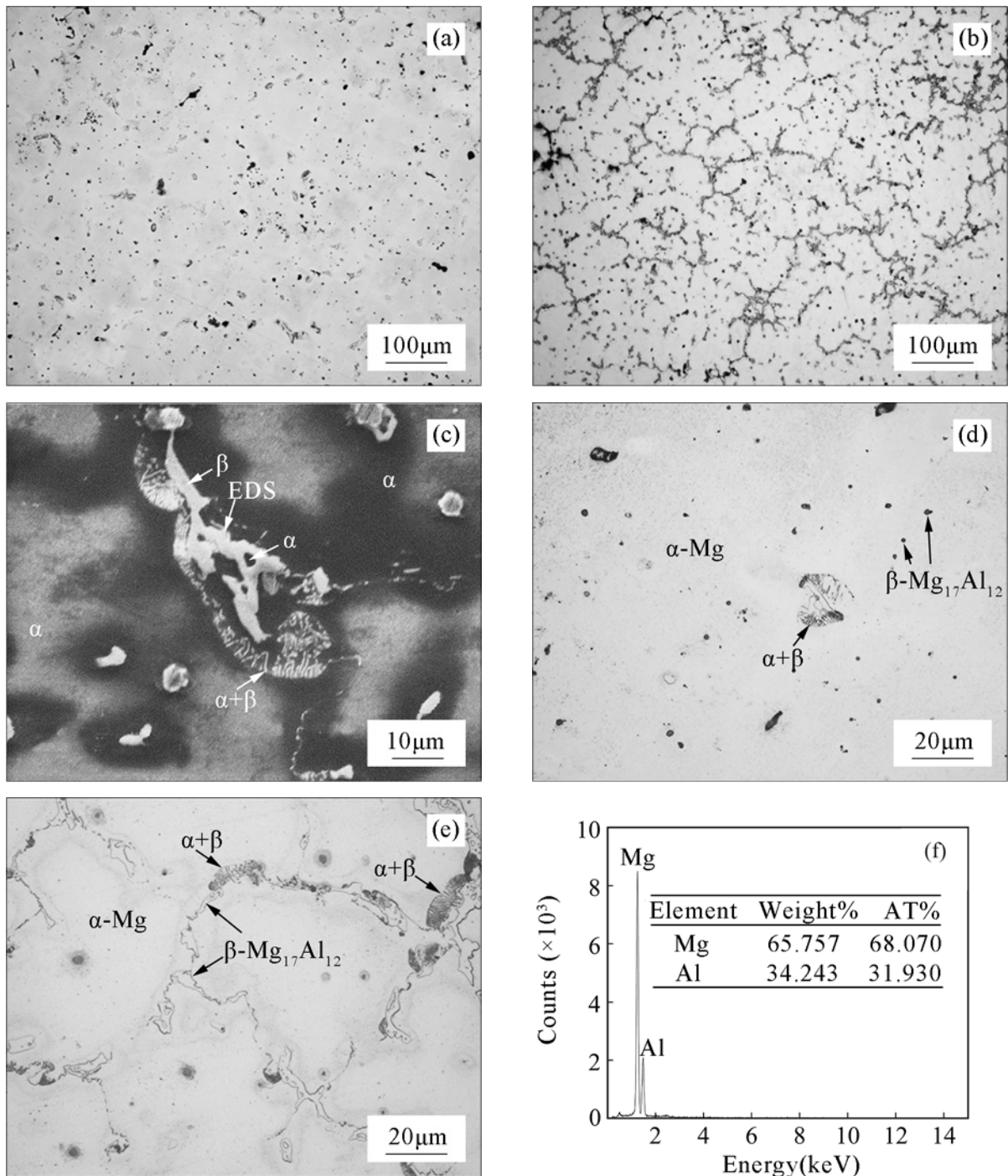


Fig. 3. The microstructure of the surfacing-welding Mg-Al-Zn alloy: (a), (d) AZ31; (b), (e) AZ91; (c) SEM micrograph of the surfacing-welding AZ91 alloy and (f) EDS result for the position labeled in Fig. 3c.

MPDDY2094, PANalytical B.V.) at an accelerating voltage of 40 kV and a current of 40 mA. The macro-hardness of the specimen was measured using a Vickers macro-hardness tester (452-SVD, Wolpert). Each specimen was measured five times, and the values were averaged.

Friction and wear tests were carried out on multifunctional friction and wear tester (MMD-1, Jinan Yihua Friction Test Technology Co., Ltd.). The pin-

-disc friction pair (Fig. 2) was utilized. The dimension of the pin was  $\varnothing 4.8 \times 12.7 \text{ mm}^2$ . Figure 1b shows the sampling position. The inner and outer diameters of the disc were 28 and 44 mm, which comprised 45 steel (hardness: 24.8 HRC). The pin and grinding disc were mechanically polished before the test, dried with ethanol, and dried. The dry sliding friction test was carried out, with a normal load of 25 N, a sliding speed of  $0.75 \text{ m s}^{-1}$ , and a sliding distance of 1 km

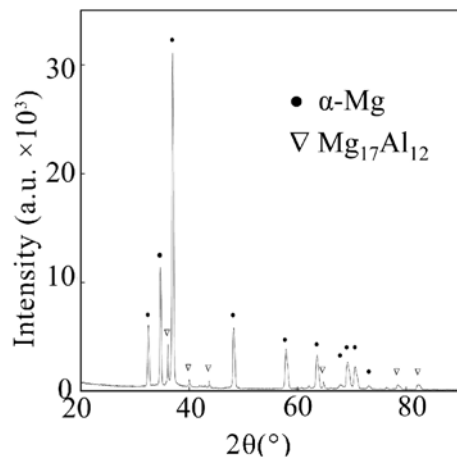


Fig. 4. XRD pattern of the surfacing-welding AZ91 alloy.

at an ambient temperature of 25 °C. The coefficient of friction (COF) can be directly read from the test instrument. The weight loss of the pin was measured by an electronic analytical balance before and after the test, and the volumetric wear rate was calculated. After the test, the worn surface and morphology of the debris were observed by SEM with energy disperse spectroscopy (EDS), and the longitudinal section microstructure of the specimen was observed by optical microscopy.

### 3. Results and discussion

#### 3.1. Microstructures

Figure 3 shows the microstructure of the surfacing-welding magnesium alloy with different Al contents. From the optical micrograph, the microstructures of the alloy mainly comprise a white  $\alpha$ -Mg matrix and a black/gray second phase. The combination of EDS results (Fig. 3f) and XRD patterns (Fig. 4) revealed that the second phase is the  $\beta$ -Mg<sub>17</sub>Al<sub>12</sub> phase. Among them, the  $\beta$ -phase in the surfacing-welding AZ31 alloy is mainly dispersed as particles. With the increase in the Al content, the amount of the  $\beta$ -phase gradually increases, and its morphology gradually changes from particles and chunks to an irregular reticular phase along the grain boundary. To better observe the morphology of the  $\beta$ -phase, further observation was performed with SEM. Figure 3c shows the SEM micrographs. A small amount of  $\alpha$ -Mg was present in the pores amidst the  $\beta$ -Mg<sub>17</sub>Al<sub>12</sub> phase, and a lamellar  $\alpha + \beta$  eutectic structure attaches to the edges.

#### 3.2. Mechanical properties

Figure 5 shows the hardness of the surfac-

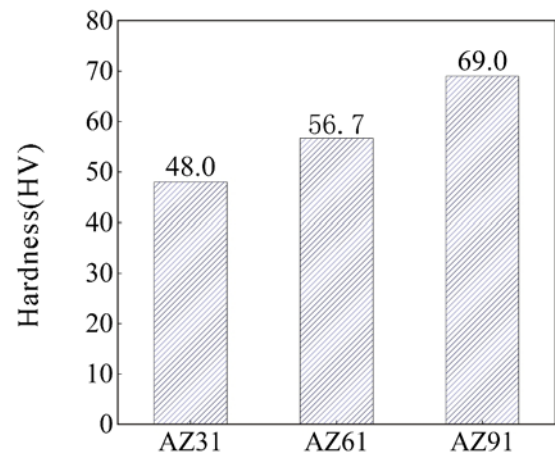


Fig. 5. The hardness of surfacing-welding alloys with different Al contents.

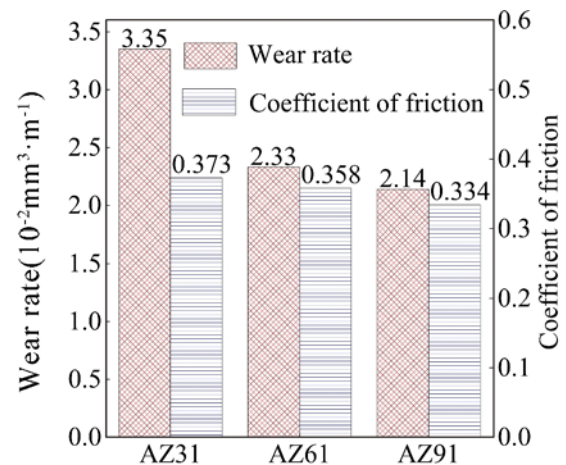


Fig. 6. COF and wear rate of surfacing-welding alloys with different Al contents.

ing-welding alloys with different Al contents. The surfacing-welding AZ31 welding wire with an Al content of 3% exhibits the lowest hardness of only 48.0 HV; with the increase in the Al content to 6%, the macro-hardness increases to 56.7 HV, with an enhancement of 8.7. Moreover, as the Al content reaches 9%, the hardness of the surfacing-welding alloy increases to the maximum value of 69.0 HV. The macro-hardness of the surfacing-welding magnesium alloy is mainly related to the amount of the  $\beta$ -phase as the  $\beta$ -phase as a hard, brittle phase exhibits a considerably higher micro-hardness than that of the Mg matrix. Therefore, with the increase in the Al content, the size and amount of the  $\beta$ -phase in the surfacing-welding magnesium alloy significantly increase (Fig. 3), as well as the hardness increases.

Figure 6 plots the statistically counted COF and wear rate of the surfacing-welding magnesium alloy. With the increase in the Al content, the trend of the

wear rate is opposite to that of hardness, and the wear resistance is gradually enhanced, which is consistent with Archard's law [16]. At an Al content of 3%, the wear rate of the surfacing-welding alloy reaches the maximum value of  $3.35 \times 10^{-2} \text{ mm}^3 \text{ m}^{-1}$ . After employing the surfacing-welding process for the AZ61 magnesium alloy wire, the wear rate rapidly decreases to  $2.33 \times 10^{-2} \text{ mm}^3 \text{ m}^{-1}$ . With the further increase in the Al content to 9%, the wear rate gradually decreases to the minimum value, but the magnitude of variation significantly decreases. The change rule of COF is similar to that of the wear rate, indicating that it decreases with the increase in the Al content, but it exhibits a lower varied extent. At an Al content of 3%, the COF of the surfacing-welding alloy reaches the maximum value of 0.373. After the increase in the Al content to 9%, the COF of the surfacing-welding alloy gradually decreases to 0.334.

The effects of the Al content on the wear resistance of the surfacing-welding alloy are mainly related to the  $\beta\text{-Mg}_{17}\text{Al}_{12}$  phase. The  $\beta$ -phase exhibits two opposite effects in the friction and wear process: on the one hand, the micro-hardness of the  $\beta$ -phase is considerably greater than that of the  $\alpha\text{-Mg}$  matrix, hence, the bulky, reticular  $\beta$ -phase can render certain protection during the wear process; resist the plowing action on matrix caused by microscopic hard protrusion and grinding debris; reduce the adverse effects of abrasive wear, and enhance the wear resistance of the alloy. On the other hand, previously, during the deformation of surface and subsurface metals caused by friction, the  $\beta$ -phases with a coarse size and an irregular shape tend to cause stress concentration and become crack sources, thereby increasing the extent of delamination wear and decreasing the wear resistance of the alloy [15, 17]. In the actual wear process, which action can dominate the variation concerning the wear resistance of magnesium alloys depends on the test parameters and micro-wear mechanism.

### 3.3. Wear mechanisms

To precisely understand the relationship between the tribological behavior of the surfacing-welding magnesium alloy and its elemental contents, the morphologies of the surface wear and debris generated after friction were observed by SEM, and then four wear mechanisms were observed: abrasive wear, oxidative wear, delamination wear, and plastic-extrusion.

Figure 7 shows the SEM images highlighting the wear morphology of the specimen surface. After the sliding friction, a large number of furrows parallel to the sliding direction are observed on the surfacing-welding AZ31 magnesium alloy surface, manifesting the main characteristics of abrasive wear. Under this wear mechanism, the microscopic hard protrusions on the grinding disc surface and the debris between fric-

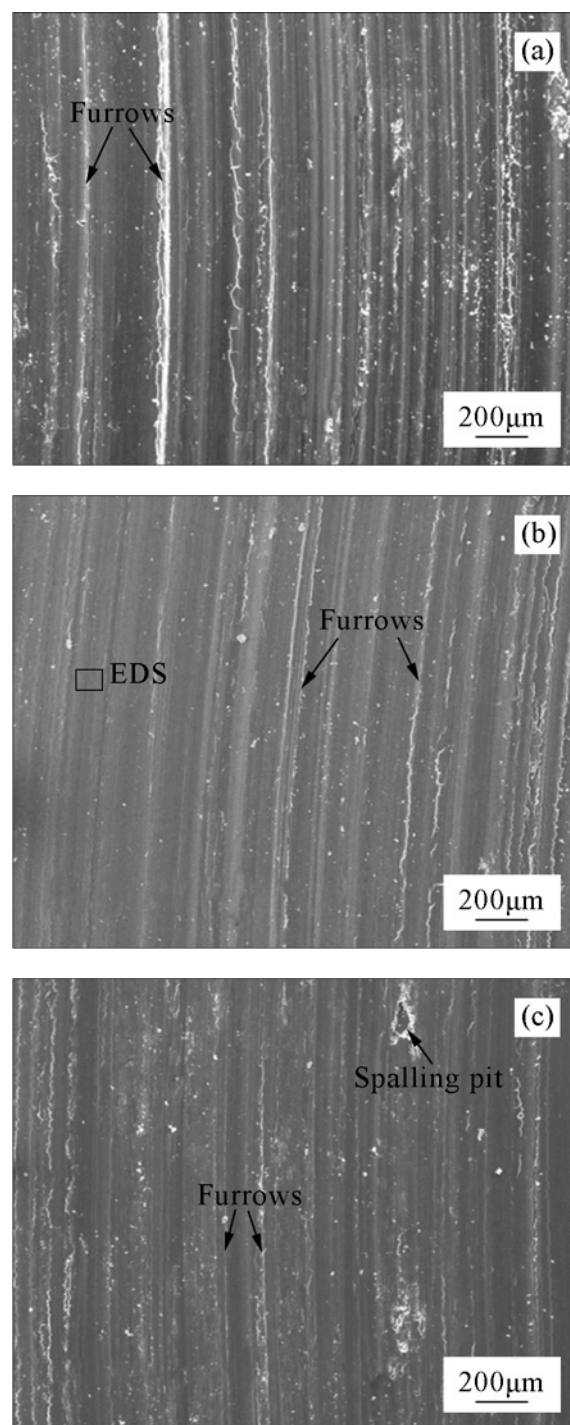


Fig. 7. Friction and wear surface morphology of surfacing-welding alloys with different Al contents: (a) AZ31, (b) AZ61, and (c) AZ91.

tion surfaces are pressed into the surface of the specimen under the test load. Next, the protrusions and debris cut and plow the surface of the specimen during sliding, leading to the breaking and falling of the surface metal and eventually forming furrows and granular wear debris (Fig. 9). Figure 7b shows the wear

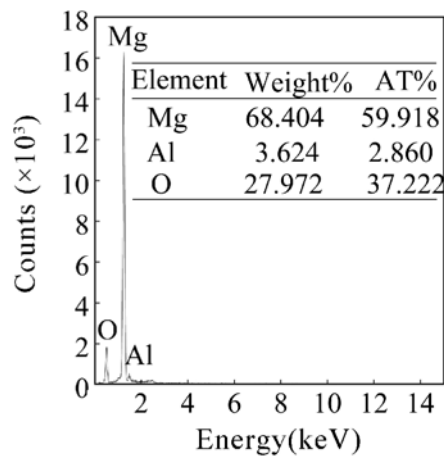


Fig. 8. EDS results for regions labeled in Fig. 7.

surface morphology of the specimen after the increase in the Al content to 6%. At this time, the number of furrows significantly decreases. With the further in-

crease in the Al content to 9%, the wear surface of the surfacing-welding alloy becomes smoother (Fig. 7c), and the extent of abrasive wear is minimized. Also, a small spalling pit is observed on the wear surface of the surfacing-welding AZ91 alloy, indicative of the delamination wear on the alloy surface. The mechanism results revealed that the surface metal is continuously subjected to the cyclic actions of the normal load and tangential friction force during the friction and wear process; the cyclic actions cause the shear deformation to occur on the surface layer and accumulate to form cracks or voids; the cracks continuously spread to the surface, eventually forming local delamination and sheet-like, block-like wear debris. However, owing to the limited test load, small spalling pit, and a lower extent of delamination wear, the delamination wear does not become the main wear mechanism. In this test, owing to the low test load, the deformed extent and depth are limited for the sub-surface metal of the surfacing-welding alloy. The principal wear mechanism is the abrasive wear, and the  $\beta$ -phase mainly serves to protect the matrix. Therefore, with the in-

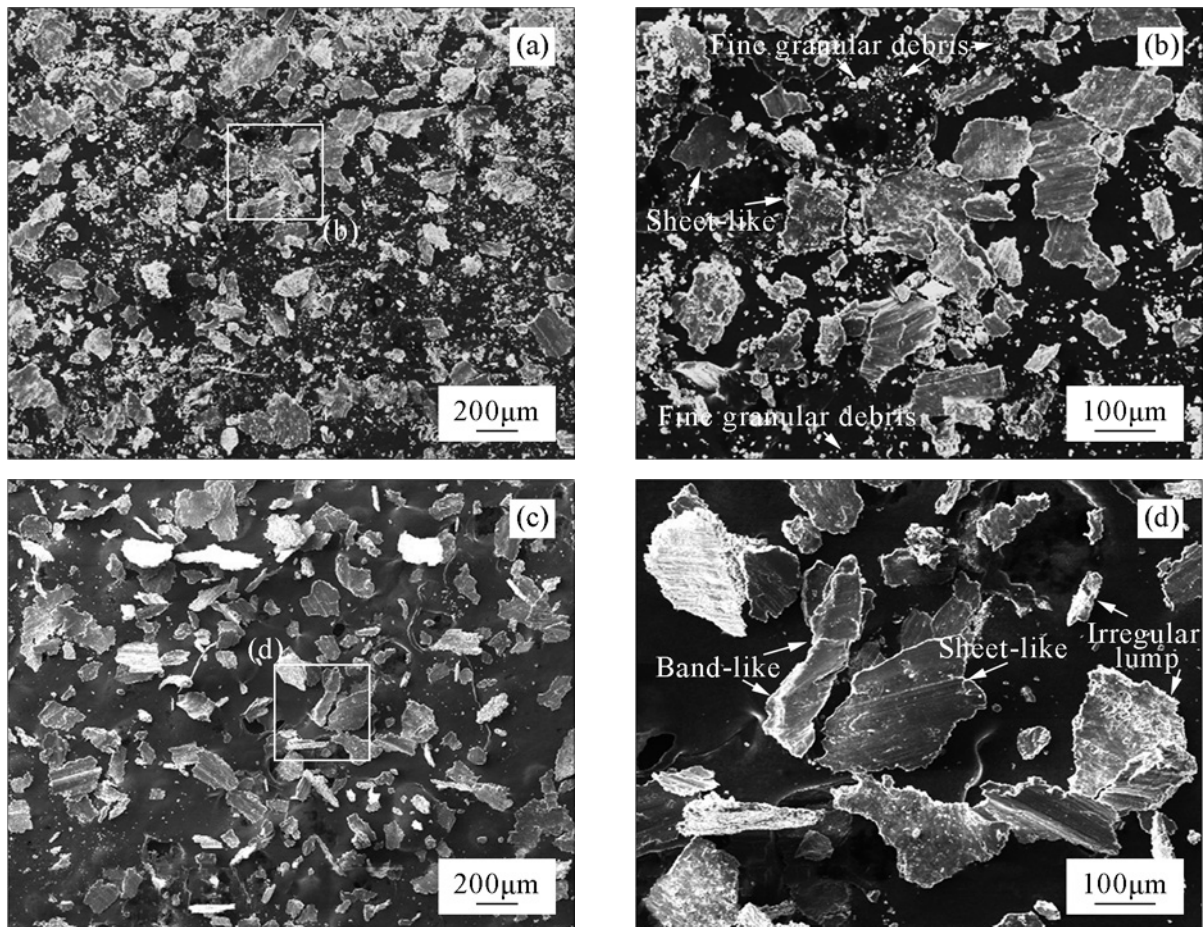


Fig. 9. Debris morphology of surfacing-welding alloys with different Al contents after friction and wear: (a), (b) AZ31 and (c), (d) AZ91.

crease in the Al content, the wear resistance of the surfacing-welding alloy gradually increases (Fig. 6).

Figure 8 shows the EDS results obtained for the elemental content of the specimen surface after friction and the wear process. A small amount of O is observed on the surfacing-welding alloy surface, indicating that the alloy also undergoes slight oxidative wear during the friction and wear process. Oxidation wear occurs because the magnesium alloy itself can be easily oxidized. Meanwhile, a large amount of friction heat is generated during friction, continuously oxidizing the alloy surface and forming an oxide film. Under the pressing and cutting actions on the metal part of the disc, the oxide film breaks and falls into granular debris; as the sliding continues, the new oxide film is regenerated and then causes wear.

Figure 9 shows the morphology of the debris after the friction and wear process. The debris of the AZ31 surfacing-welding alloy mainly comprises fine granular debris and large pieces of flaky wear debris. Among them, fine granular debris mainly originates from abrasive wear. With the increase in the Al content to 9%, the abrasive wear extent of the AZ91 surfacing-welding alloy decreases (Fig. 7); hence, the number of fine debris in Figs. 9c,d significantly decrease. Also, a large amount of flaky wear debris is observed (Fig. 9). Generally, the flaky wear debris is mainly related to the overall peeling of the surface metal caused by the delamination wear. However, in the test, the extent of delamination wear is low for these alloy systems (Fig. 7), and a limited amount of wear debris is generated by this mechanism. At the same time, the edge morphology of the surfacing-welding alloy after wear revealed a large number of lamellar structures (Fig. 10). Therefore, flaky debris is considered to result from the plastic-extrusion mechanism of the surface metal mainly, that is, during sliding friction, the friction-generated heat and the friction force act together and cause the thermal softening and severe plastic deformation of the surface metal (Fig. 10b). Furthermore, the softened, deformed surface metal is continuously squeezed to the edge of the specimen, extruded, and peeled off to form flaky and chunky debris [18]. Finally, a lamellar structure is formed at the edges of the test pin.

#### 4. Conclusions

In this study, the surfacing-welding process of the Mg-Al-Zn alloy wire with different Al contents was carried out, and the friction and wear behavior of the welding wire were examined by the pin-disc dry friction and wear test at room temperature. The conclusions are as follows:

1. With the increase in the Al content from 3 to 9%, the macro-hardness of the surfacing-welding

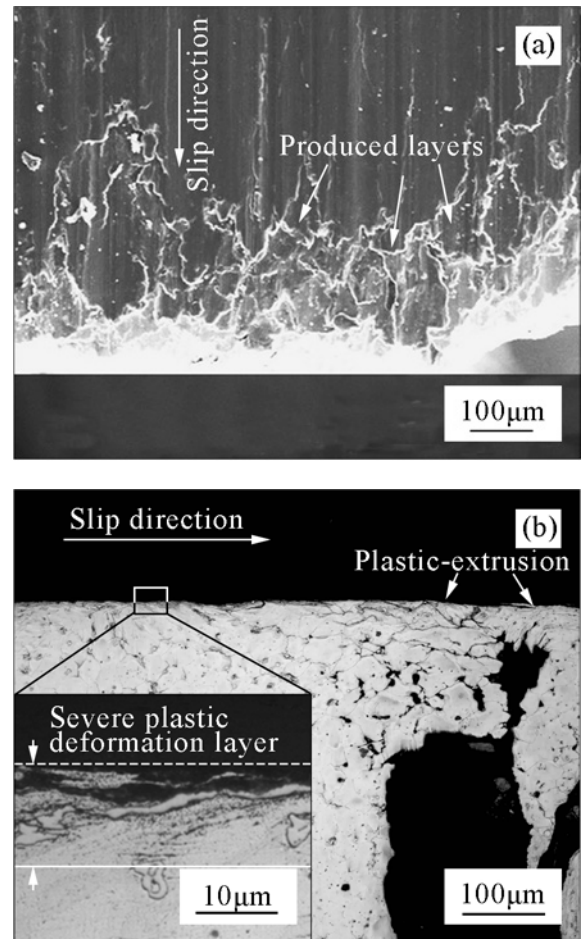


Fig. 10. Morphology of the worn edge of the surfacing-welding AZ61 alloy: (a) SEM image and (b) optical microstructure of the longitudinal section.

Mg-Al-Zn alloy gradually increases, and the COF and wear rate gradually decrease. Among them, the surfacing-welding AZ91 alloy with an Al content of 9% exhibits the lowest wear rate and the best wear resistance.

2. Under the test conditions, the effect of the Al content on the wear resistance of the surfacing-welding Mg-Al-Zn alloy is mainly related to the size and amount of the  $\beta$ -Mg<sub>17</sub>Al<sub>12</sub> phase. With the increase in the Al content, the size and number of the  $\beta$ -phase gradually increase. Meanwhile, the morphology of the  $\beta$ -Mg<sub>17</sub>Al<sub>12</sub> phase evolves from the dispersed particles to a reticular structure, which can protect the matrix during the wear process, resist the ploughing actions caused by microscopic hard protrusions and wear debris, decrease the amount of fine granular debris generated by the abrasive wear mechanism, and enhance the wear resistance of the surfacing-welding alloy.

3. Under the test conditions, four wear mechanisms are observed during the friction process of the surfacing-welding Mg-Al-Zn alloy: abrasive wear, ox-

idative wear, delamination wear, and severe plastic deformation. Among these wear mechanisms, abrasive wear and severe plastic deformation are the principal wear mechanisms.

### Acknowledgements

This work was supported by the PhD Research Foundation of Shandong Jianzhu University (XNBS1807), National Natural Science Foundation of China (51605262), Shandong Provincial Natural Science Foundation (ZR2019BEE033).

### References

- [1] T. M. Pollock, Weight Loss with Magnesium Alloys, *Science* 328 (2010) 986–987. [doi:10.1126/science.1182848](https://doi.org/10.1126/science.1182848)
- [2] Z. Zeng, N. Stanford, C. H. J. Davies, J.-F. Nie, N. Birbilis, Magnesium extrusion alloys: a review of developments and prospects, *Int. Mater. Rev.* 64 (2019) 27–62. [doi:10.1080/09506608.2017.1421439](https://doi.org/10.1080/09506608.2017.1421439)
- [3] Y. Li, F. Qin, C. Liu, L. Li, X. Zhao, Z. Wu, Influence of Annealing Treatment on Microstructure Evolution and Mechanical Property of Friction Stir Weld AZ31 Mg Alloys, *J. Wuhan Univ. Technol.* 34 (2019) 417–425. [doi:10.1007/s11595-019-2068-0](https://doi.org/10.1007/s11595-019-2068-0)
- [4] B. Song, C. Wang, N. Guo, H. Pan, R. Xin, Improving Tensile and Compressive Properties of an Extruded AZ91 Rod by the Combined Use of Torsion Deformation and Aging Treatment, *Materials* 10 (2017) E280. [doi:10.3390/ma10030280](https://doi.org/10.3390/ma10030280)
- [5] M. De Souza Elias, R. Paranhos, Metallurgical evaluation of austenitic stainless surfacing welding on SAE 4130 steel, *Welding International* 30 (2016) 581–589. [doi:10.1080/09507116.2015.1096559](https://doi.org/10.1080/09507116.2015.1096559)
- [6] S. Zhu, C. Li, C. D. Shen, J. Liu, Microstructure and Micro Mechanical Property of Part Formed by GMAW Surfacing Rapid Prototyping, *Key Engineering Materials* 419–420 (2009) 853–856. [doi:10.4028/www.scientific.net/KEM.419-420.853](https://doi.org/10.4028/www.scientific.net/KEM.419-420.853)
- [7] S. Zhu, Q. W. Wang, F. L. Yin, Y. Y. Liang, L. Chen, Influence of Alternative Magnetic Field Frequency on Microstructure and Properties of Surfacing Welding Layer of Aluminum Alloy, *Materials Science Forum* 697–698 (2011) 351–355. [doi:10.4028/www.scientific.net/MSF.697-698.351](https://doi.org/10.4028/www.scientific.net/MSF.697-698.351)
- [8] X. D. Niu, D. Q. An, X. Han, W. Sun, T. F. Su, J. An, R. G. Li, Effects of Loading and Sliding Speed on the Dry Sliding Wear Behavior of Mg-3Al-0.4Si Magnesium Alloy, *Tribol. T.* 60 (2017) 238–248. [doi:10.1080/10402004.2016.1158890](https://doi.org/10.1080/10402004.2016.1158890)
- [9] J. An, Y. X. Zhang, X. X. Lv, Tribological Characteristics of Mg-3Al-0.4Si-0.1Zn Alloy at Elevated Temperatures of 50–200 °C, *Tribol. Lett.* 66 (2018) 14. [doi:10.1007/s11249-017-0968-8](https://doi.org/10.1007/s11249-017-0968-8)
- [10] H. J. Hu, Z. Sun, Z. W. Ou, X. Q. Wang, Wear behaviors and wear mechanisms of wrought magnesium alloy AZ31 fabricated by extrusion-shear, *Eng. Fail. Anal.* 72 (2017) 25–33. [doi:10.1016/j.engfailanal.2016.11.014](https://doi.org/10.1016/j.engfailanal.2016.11.014)
- [11] P. Seenuvasaperumal, K. Doi, D. A. Basha, A. Singh, A. Elayaperumal, K. Tsuchiya, Wear behavior of HPT processed UFG AZ31B magnesium alloy, *Mater. Lett.* 227 (2018) 194–198. [doi:10.1016/j.matlet.2018.05.076](https://doi.org/10.1016/j.matlet.2018.05.076)
- [12] K. R. Athul, A. Srinivasan, U. T. S. Pillai, Investigations on the microstructure, mechanical, corrosion and wear properties of Mg-9Al-xGd (0, 0.5, 1, and 2 wt.%) alloys, *J. Mater. Res.* 32 (2017) 3732–3743. [doi:10.1557/jmr.2017.348](https://doi.org/10.1557/jmr.2017.348)
- [13] H. R. Jafari Nodooshan, W. Liu, G. Wu, W. Ding, R. Mahmudi, Effect of Gd addition on the wear behavior of Mg-xGd-3Y-0.5Zr alloys, *J. Mater. Res.* 31 (2016) 1133–1144. [doi:10.1557/jmr.2016.113](https://doi.org/10.1557/jmr.2016.113)
- [14] H. Yan, Z. Wang, Effect of heat treatment on wear properties of extruded AZ91 alloy treated with yttrium, *J. Rare Earths* 34 (2016) 308–314. [doi:10.1016/S1002-0721\(16\)60030-3](https://doi.org/10.1016/S1002-0721(16)60030-3)
- [15] Q. Q. Chen, Z. H. Zhao, Q. F. Zhu, G. S. Wang, K. Tao, Cerium Addition Improved the Dry Sliding Wear Resistance of Surface Welding AZ91 Alloy, *Materials* 11 (2018) E250. [doi:10.3390/ma11020250](https://doi.org/10.3390/ma11020250)
- [16] J. F. Archard, Contact and Rubbing of Flat Surfaces, *J. Appl. Phys.* 24 (1953) 981–988. [doi:10.1063/1.1721448](https://doi.org/10.1063/1.1721448)
- [17] Q. Q. Chen, Z. H. Zhao, Q. F. Zhu, G. S. Wang, K. Tao, Effects of heat treatment on the wear behavior of surfacing AZ91 magnesium alloy, *J. Mater. Res.* 32 (2017) 2161–2168. [doi:10.1557/jmr.2017.186](https://doi.org/10.1557/jmr.2017.186)
- [18] J. Zhang, X. Zhang, Q. Liu, S. Yang, Z. Wang, Effects of Load on Dry Sliding Wear Behavior of Mg-Gd-Zn-Zr Alloys, *J. Mater. Sci. Technol.* 33 (2017) 645–651. [doi:10.1016/j.jmst.2016.11.014](https://doi.org/10.1016/j.jmst.2016.11.014)